Chemical Engineering Science 68 (2012) 94–100

Contents lists available at SciVerse ScienceDirect

Chemical Engineering Science

journal homepage: www.elsevier.com/locate/ces

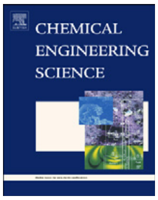

Supercritical CO_2-assisted preparation of a PMMA composite membrane for bisphenol A recognition in aqueous environment

Mara Soares da Silva, Raquel Viveiros, Mónica B. Coelho, Ana Aguiar-Ricardo, Teresa Casimiro*

REQUIMTE, Departamento de Química, Faculdade de Ciências e Tecnologia, FCT, Universidade Nova de Lisboa, 2829-516 Caparica, Portugal

ARTICLE INFO

Article history:
Received 24 May 2011
Received in revised form
1 September 2011
Accepted 7 September 2011
Available online 22 September 2011

Keywords:
Supercritical carbon dioxide
Membrane technology
Molecularly imprinted polymers
Immobilization
Composite membrane
Adsorption

ABSTRACT

This work reports a novel strategy to prepare affinity composite membranes using supercritical fluid technology. By blending molecularly imprinted polymeric particles with PMMA, a porous hybrid structure with affinity to the template molecule, bisphenol A, was prepared using a supercritical carbon dioxide ($scCO_2$)-assisted method. Membranes were characterized in terms of morphology, mechanical performance and transport properties. The ability of the polymers and hybrid membranes to adsorb bisphenol A was tested in aqueous solutions and fitted to a linearized Langmuir equation, showing that adsorption takes place at homogeneous affinity binding sites within the imprinted surface. Filtration experiments showed that the imprinted hybrid membrane was able to adsorb higher amounts of template even in non-equilibrium dynamic binding conditions. The hybridization of the PMMA membrane herein reported conveys two important improvements over neat PMMA membrane: it introduced molecular affinity towards the template molecule and significantly increased the permeability of the porous structures, which are key parameters in processes that involve membranes. This technique could expand the applications of polymeric beads powders and enhance the efficiency of the membrane's transport properties. Our work presents a new method to confer affinity to a porous structure by immobilization of imprinted polymers, combining polymer synthesis and membrane formation using supercritical fluid technology.

1. Introduction

Over the last years, there has been a growing interest in the design and development of advanced polymeric materials using clean and sustainable technologies. In this context, ever since the first work concerning the preparation of membranes by $scCO_2$-assisted phase inversion method was reported (Kho et al., 2001) others have recognized its potential (Temtem et al., 2009; Reverchon and Cardea, 2004; Reverchon et al., 2006). The preparation of membranes using this technology encounters numerous advantages due to the tuneable properties of supercritical carbon dioxide. In the vicinity of the critical point, a small variation in pressure leads to a sharp increase in density and therefore in the solvent strength. Given the non-solvent role of CO_2 in the phase inversion process, a variation in its density alters the phase diagram of the ternary system polymer/solvent/non-solvent and enables to control the membrane characteristics through the non-solvent effect (Reverchon and Cardea, 2004, 2006; Matsuyama et al., 2001). The production of membranes by this method introduces new experimental parameters (temperature, pressure and depressurization rate) over the traditional process variables (polymer concentration, solvent), allowing a higher control of the morphology and porosity. This can be a powerful tool in the design of porous structures for effective processes in filtration (Van der Mare et al., 2010) and sensing (Wang et al., 2010).

New trends in membrane technology encounter the development of affinity membranes with inherent high-throughputs. The design of affinity membranes with molecular recognition character is inspired in natural mechanisms. Molecularly imprinted membranes emerge as potential affinity materials due to their low cost, ease of preparation and good molecular recognition performance. The concept of creating affinity sites in a molecularly imprinted membrane lays in the molecular imprinting mechanism. Imprinting of molecules is achieved by polymerization of functional monomers and cross-linking agent in the presence of the template molecule. As template and monomers establish interaction complexes, these become spatially fixed into a solid matrix by polymerization and the polymer chains grow with a certain controlled conformation. Template desorption at the end of the polymerization leaves accessible the highly specific molecular recognition sites that are complementary in size, shape and chemical functionality.

Over the last years, molecular recognition polymers have found many applications in a wide variety of areas such as in sensors

---

* Corresponding author. Tel.: +351 212948385; fax: +351 212948550.
E-mail address: teresa.casimiro@dq.fct.unl.pt (T. Casimiro).
URL: http://www.dq.fct.unl.pt/scf/.

0009-2509/$ - see front matter © 2011 Elsevier Ltd. All rights reserved.
doi:10.1016/j.ces.2011.09.015

(Moreira et al., 2010), solid-phase extraction (Beltran et al., 2010), chromatography (Amut et al., 2009) and drug delivery (Kryscio and Peppas, 2009) due to their high affinity and chemical, mechanical and thermal stability. The most commonly applied molecularly imprinted polymer (MIP) synthesis procedure is bulk synthesis, which results in a hard block polymer that must be grinded and sieved. Besides time-consuming, this method gives rise to several drawbacks, namely, irregular particles, destroyed interaction sites, slow interaction kinetics, heterogeneous geometry and poor accessibility of the binding sites (Qiao et al., 2006; Alexander et al., 2003). Other methods have been reported, but the persistence of several drawbacks and the use of hazardous organic solvents limit a more wide acceptance and application of MIPs (Wei and Mizaikoff, 2007).

Supercritical fluids have emerged as a viable alternative to traditional organic solvents because of their physical and chemical properties. Supercritical carbon dioxide, in particular, is the most applied supercritical fluid for polymerization reactions, because of its numerous advantages: it is non-toxic, non-flammable, is a by-product of industrial processes, has low critical point and reverts to the gaseous state upon depressurization, simplifying the separation of solvent from solute and eliminating solvent residues (Cooper and Holmes, 1999; de Macedo et al., 2007). Recently we have proven that $scCO_2$ is a suitable porogen for molecular imprinting by synthesizing high affinity MIPs with attested performance in drug delivery and chiral chromatography (Duarte et al., 2006; Soares da Silva et al., 2011, 2010). When developing a successful imprinted matrix, the porogen solvent is one of the most important factors determining effective molecular recognition. By performing the synthesis in an apolar aprotic porogen, such as $scCO_2$, the template–monomer complexes are highly stable giving rise to materials with high affinity. Furthermore, MIPs synthesized using supercritical fluid technologies are obtained as free-flowing powders with controlled morphology and porosity.

In literature we could found several works concerning the development of molecularly imprinted membranes (Sergeyeva et al., 2003; Donato et al., 2010; Hattori et al., 2004; Kobayashi et al., 2008). However, much has to be done to rationally design valuable molecularly imprinted membranes. To the best of our knowledge, the incorporation of pre-synthesized MIPs in a casting solution for membrane preparation has been reported only few times up to now (Takeda et al., 2005). In analogy to the already marketed SPE membranes, this approach could open further possibilities for the design of molecular recognition structures (Ulbricht, 2004). The development of hybrid membranes using supercritical fluid technology could yield affinity membranes with controlled porosity and permeability combined to the green aspects of this clean technology, both in terms of purity and process sustainability.

This work describes the successful immobilization of highly cross-linked polymeric particles with affinity to bisphenol A, BPA, into a PMMA-based porous structure, by blending the synthesized imprinted polymer within a PMMA casting solution, followed by $scCO_2$-assisted phase inversion. Fig. 1 schematizes the experimental procedure employed in this work.

BPA is an endocrine disruptor that is intensively used in the production of polycarbonate plastics and resins. With a worldwide production of approximately 2.2 million tonnes in 2009, it is one of the highest volume chemicals in commerce (Burridge, 2003), although it is known that small daily doses of exposure to BPA are known to increase the risk of breast and prostate cancer (Dairkee et al., 2008) and diabetes (Lang et al. 2008). The proposed devices could have a real application in BPA adsorption by combining a completely pure and solvent-free material with enhanced affinity to adsorb this molecule.

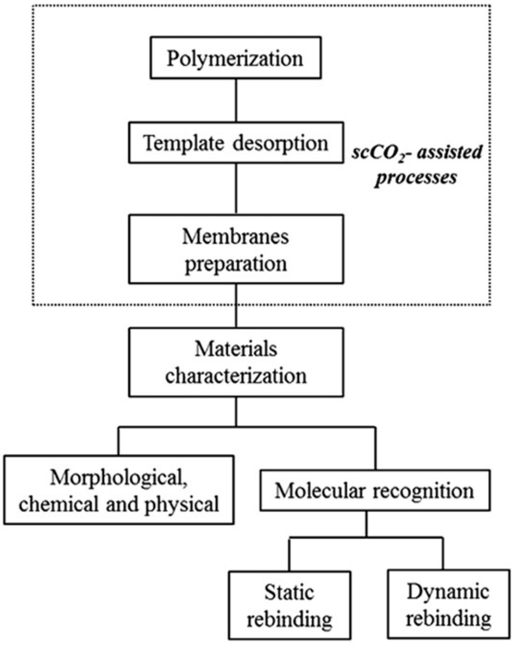

Fig. 1. Scheme of the experimental procedure used in this work.

We envisage that several fields, in a near future, could benefit with the morphology, affinity and purity of the porous structures prepared using this green technology.

2. Experimental

2.1. Materials

Bisphenol A (BPA, 99% purity) as template, methacrylic acid (MAA, 99% purity) as functional monomer and ethylene glycol dimethacrylate (EGDMA, 98% purity) as cross-linker were purchased from Sigma-Aldrich; Azobis(isobutyronitrile) (AIBN, 98% purity) from Fluka was used as initiator. Poly(methyl methacrylate) (PMMA) (molecular weight 996,000) was obtained from Sigma-Aldrich. Dimethylformamide (DMF, 99.8% purity) was purchased from Riedel-de Haën and ethanol (PA) from Panreac. Methanol isocratic HPLC grade (99.7% purity) from Scharlau was used. Carbon dioxide was obtained from Air Liquide with purity better than 99.998%. All chemicals were used without further purification.

2.2. MIP and NIP synthesis in $scCO_2$

Polymerization reactions in $scCO_2$ were carried out as described elsewhere (Casimiro et al., 2005). In a typical procedure to synthesize the non-covalent MIP, 0.49 mmoles of the template molecule BPA, 2.54 mmoles of the functional monomer MAA, 12.88 mmoles of the cross-linker agent EGDMA (molar ratios 1:5:25) and 1 wt% of the radical initiator AIBN were introduced in a 33 mL stainless steel high-pressure cell equipped with two aligned sapphire windows and a Teflon coated magnetic stir bar inside. The cell was immersed in a thermostated water bath at 65 °C, the optimal AIBN initiation temperature, and temperature control was made through an open bath circulator Julabo Ed with stability ± 0.1 °C. Carbon dioxide was added up to 21 MPa and polymerization reactions proceeded for 24 h under stirring. At these initial temperature and pressure conditions, a single homogeneous phase is assured, with all reactants completely dissolved in the supercritical phase. At the end of the reaction, the polymer was slowly washed with fresh high-pressure CO_2 for 1 h in order to remove the template molecule and wash any unreacted residues. For the synthesis of the non-imprinted polymer (NIP) the same procedure was followed except no template was added.

2.3. $scCO_2$-assisted template desorption

Template desorption from the imprinted matrices at the end of the polymerization is a crucial step in the molecular imprinting process because the formerly created binding sites have to be emptied to become available for future rebinding. The use of supercritical fluids to remove the template from imprinted matrices can increase the diffusion coefficient at least 10-fold, with higher template desorption being achieved for relatively non-polar compounds (Ellwanger et al., 2001). $ScCO_2$-assisted BPA desorption was performed by loading a 33 mL stainless steel high-pressure cell with 1.5 g of the pre-synthesized polymer, 10 mL of methanol and CO_2 until 21 MPa was reached. The cell was immersed in a thermostated water bath at 40 °C and 24 h. The polymer was then slowly washed for 3 h with fresh high-pressure CO_2 in order to remove all the template and co-solvent. The residual amount of BPA entrapped in the highly cross-linked matrix was assessed by crushing 20 mg of polymer, stirring it with 3 mL of methanol for 3 days and quantifying the template amount that was released by UV spectroscopy. BPA calibration curves were performed in a Perkin-Elmer λ 25 spectrometer at 275 nm.

2.4. $scCO_2$-assisted production of hybrid molecularly imprinted membrane

The production of molecularly imprinted supported membranes by $scCO_2$-assisted phase-inversion was carried out in a high-pressure apparatus already described elsewhere (Temtem et al., 2006, 2008) in a high-pressure cell specially developed for membrane production. Briefly, to produce the membranes, the casting solution with 30 wt% of polymer blend consisting in 70:30 of PMMA and MIPs or NIP, in 5 mL of DMF, was loaded into a teflon cap and placed inside the high-pressure cell. The cell has a porous structure that supports a bed of Raschig rings, in order to disperse CO_2 in the top of the casting solution. Membrane production was performed at 45 °C by immersing the cell in a thermostated water bath, heated by means of a controller (Hart Scientific, Model 2200) that maintained the temperature within ± 0.01 °C. CO_2 was added, using a Gilson 305 piston pump, until an operational pressure of 20 MPa was reached. Pressure was set at 20 MPa by means of a back pressure regulator (Jasco BP-2080 plus), which separates the CO_2 from the DMF present in the casting solution. All the experiments were performed with a CO_2 flow of 9.8 g min^{-1} for 3 h. The pressure inside the system is monitored with a pressure transducer (Setra Systems Inc, Model 204) with a precision of ± 0.100 kPa. At the end, the system was slowly depressurized during 20 min and a thin homogeneous membrane composed of PMMA and MIP (PMMA MIP) or NIP (PMMA NIP) was obtained. The pure PMMA membrane was prepared using the same procedure except that no pre-synthesized polymer was added to the casting solution.

2.5. Morphological, chemical and physical characterization of imprinted materials

Imprinted materials were characterized in terms of morphology using scanning electron microscopy (SEM) in a Hitachi S-2400 instrument, with an accelerating voltage set to 15 kV. For cross-section analysis the membrane samples were frozen and fractured in liquid nitrogen. Samples were mounted on aluminum stubs using carbon tape and were gold coated. Specific surface area and pore diameter of polymer powders were determined by N_2 adsorption according to the BET method. An accelerated surface area and porosimetry system (ASAP 2010 Micromeritics) was used under nitrogen flow. Fourier transform infrared spectroscopy (FTIR) analysis measurements were performed using a Bruker Tensor 27 (16 scans and 1 cm^{-1} resolution). Pellets containing finely grounded powder of a small amount of each copolymer mixed with dried KBr (1:5 mass ratio) were made before recording. Differential scanning calorimetry (DSC) experiments of the produced MIP particles and PMMA and PMMA+ MIPs membranes using a Setaram (Model DSC 131) equipment. The analyses were performed from 0 to 350 °C at 5 °C/min under dry nitrogen atmosphere.

The hydrophobicity of the membranes was evaluated through the measurement of the contact angles with Millipore water droplets in a KSV Goniometer model CAM 100 at room temperature. The permeability of the membranes to pure water was determined by measuring the water flux through the membranes using a 10 mL filtration unit (Amicon Corp., model 8010) with an effective area of 4.1 cm^2. All the experiments were carried out varying the applied hydrostatic pressure from 0 to 0.50 MPa.

The tensile properties of the membranes were tested by dynamic mechanical analysis (DMA) with a tensile testing machine (MINIMAT firm-ware v.3.1) at room temperature. The samples were cut into 5 mm × 15 mm strips. The length between the clamps was set at 5 mm and the speed of testing was set to 0.1 mm min^{-1}. A full scale load of 20 N and maximum extension of 35 mm were used. Measurements were performed with dried membranes. The Young modulus was calculated from the slope of the linear portion of the stress–strain curve. All samples were tested in dry state at room temperature. Load extension graphs were obtained during testing and converted to stress–strain curves through Eqs. (1) and (2), with σ being the stress (N mm^{-2}), F the applied force (N), A the cross sectional area (mm^2), ε the strain, ΔL the change in length (mm) and L the length between clamps (mm):

$$\sigma = \frac{F}{A} \tag{1}$$

$$\varepsilon = \frac{\Delta L}{L} \tag{2}$$

2.6. Template static adsorption experiments

Batch binding experiments were carried out to evaluate the static adsorption capacity of the synthesized polymers and membranes by adding 20 mg of polymeric material MIP, its corresponding blank polymer, NIP, PMMA membrane and its corresponding blends of PMMA MIP and PMMA NIP in 50 mL volume of aqueous solution of BPA, stirred at 50 rpm, with concentrations ranging from 50 to 300 μM. Equilibrium was achieved after 24 h, as confirmed by the quantification of free BPA in solutions. The amount of substrate adsorbed by the matrices was assessed through Eq. (3), where $[S]$ corresponds to the amount of BPA bound, C_0 represents the initial molar concentrations of BPA, C_t corresponds to the concentrations at predetermined time intervals, V represents the volume of the solution and W corresponds to the weight of the polymeric sample:

$$[S] = \frac{(C_0 - C_t)V}{W} \tag{3}$$

2.7. Template dynamic binding

To assess the performance of the imprinted membrane in adsorbing the template molecule at dynamic conditions, the membrane was put in the permeability apparatus and electrostatic pressure was adjusted to assure a constant filtration flow rate of 0.33 mL min^{-1}. Previous to the adsorption experiments, the membrane was equilibrated with 30 mL (3 mL × 10 mL) of distilled water. The filtration unit was then loaded with 30 mL of an aqueous solution containing 300 μM of BPA and the amount of template adsorbed in the imprinted membrane was quantified. The membrane was easily restored by washing it with 10 mL of methanol at the same flow rate and no loss of binding capacity was observed. As control, the non-imprinted hybrid membrane was also studied with respect to its ability to bind the template in non-equilibrium conditions. All samples collected were quantified by UV spectroscopy. The amount of BPA bound to the membranes was determined using Eq. (3).

3. Results and discussion

3.1. Morphologic, chemical and physical characterization

Imprinted and non-imprinted polymers were obtained as dry, free-flowing powders in high yields (~99%, determined gravimetrically). These yields are in accordance with other reported precipitation polymerizations in scCO$_2$ (Cao and Chen, 2006). The synthesis and processing of MIPs in scCO$_2$ offers numerous advantages over traditional methods; besides the high stabilization of the template–monomer complex and the inexistence of traces of solvent, the imprinted polymers synthesized in scCO$_2$ do not need to be grounded and sieved prior to use, therefore avoiding posterior time-consuming steps and partial destruction of the recognition sites. The immobilization of highly cross-linked particles in an acrylate-based membrane cast was successfully achieved, which can be explained by the similar structures of P(MAA-co-EGDMA) and PMMA, as the incorporation of the same polymeric particles in a polysulfone-based membrane, in a first approach, led to distinct segregation of the two polymers and therefore make that system impossible to study. Successful hybridization was assessed by gravimetric analysis, with the membrane dry, before and after water elution in the filtration cell and visually by SEM.

The morphology of the polymeric materials used in this work was evaluated through scanning electron microscopy. Fig. 2 presents the SEM images of imprinted polymer, and neat and hybrid PMMA porous structures. SEM image of the synthesized polymers show aggregates of smooth surfaced discrete nanoparticles, with imprinted and blank polymer presenting similar morphology. Using scCO$_2$-assisted phase inversion method to prepare membranes, homogeneous structures are obtained, as it can be confirmed by SEM images. The pure PMMA membrane produced herein possesses a homogeneous morphology with low porosity on the top layer of the membrane and regular pores across the structure. By SEM images it is possible to assess the hybridization of the matrices and the influence of incorporating cross-linked particles in the morphology of the membranes. Hybrid membranes present spherical and regular pores in the top and across the membrane and a homogeneous distribution of pre-synthesized polymeric particles over the membrane scaffold. The introduction of the highly cross-linked particles in the PMMA membrane cast does not seem to have a significant effect on the pore size, but significantly changes the top surface of the structure, with hybrid membranes possessing higher roughness and a higher amount of pores.

FTIR analysis was performed to both synthesized polymers and membranes (data not shown) and the characteristic bands of methacrylic acid and methacrylate were identified at the respective wavenumber. The carbonyl stretching absorption by free carbonyl groups for methacrylate units is described at 1730 cm^{-1} whilst the carbonyl stretching bands of methacrylic acid range from 1742 to 1699 cm^{-1}, according if the groups are free or hydrogen bonded, respectively. In this work NIP and MIP are copolymers of MAA and EGDMA, in the molar ratio of 1:5 and the stretching absorption of carbonyl appears at 1728 cm^{-1}. In agreement with the same composition, NIP and template-desorpted MIP present similar spectra. The incorporation of NIP and MIP in the scaffold of PMMA membranes was not possible to

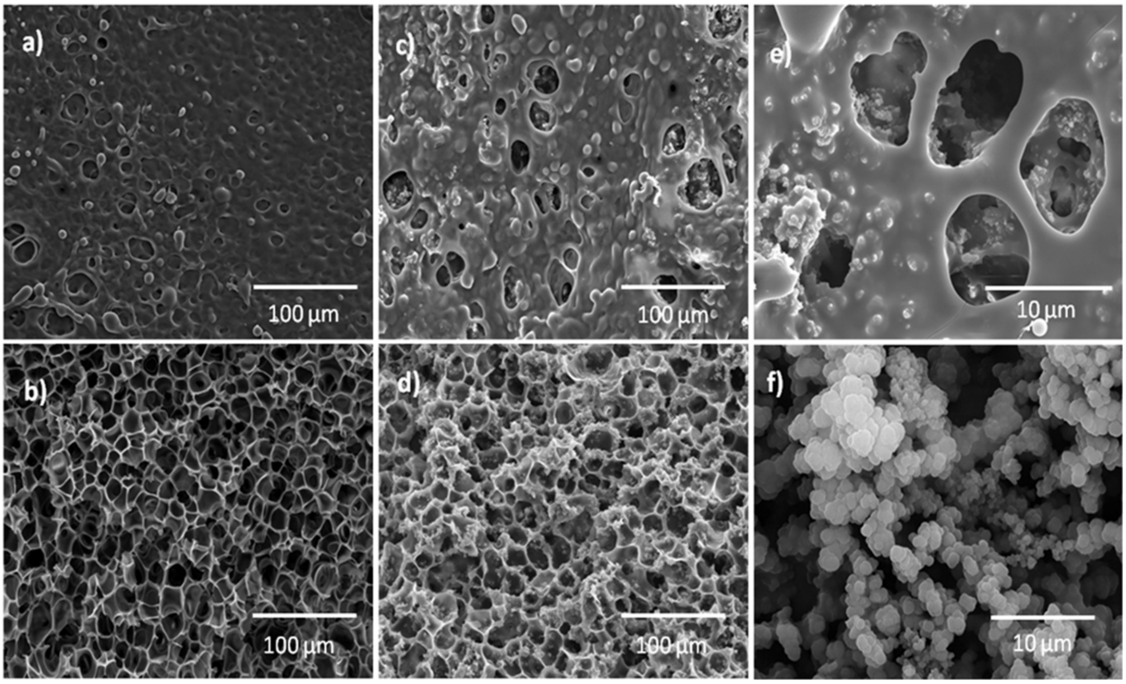

Fig. 2. Scanning electron micrograph images of the developed structures: (a) top surface and (b) cross section of PMMA membrane, (c) top surface and (d) cross section of PMMA MIP hybrid membrane, (e) detail of the top surface of PMMA MIP, (f) MIP.

assess by the analysis of FTIR spectra as the carbonyl stretching of PMMA and hybrid PMMA membranes appear both at 1734 cm^{-1}.

From DSC experiments it was possible to conclude that the PMMA membrane has a thermal pattern in accordance with a semi-crystalline polymer with amorphous and crystalline moieties, showing a T_g around 106 °C and a melting point temperature of around 133 °C. As expected, MIP and NIP are amorphous materials, typical of the polymers synthesized in supercritical CO_2. Because of their reduced polymer chain mobility, due to their highly cross-linked nature, no variation in the heat flow was observed, and hence no T_g was detected. Also no significant changes in the DSC thermograms of the hybrid PMMA membranes were observed when compared with the neat PMMA membrane. No T_g was detected but a T_m at 133 °C was also found in the hybrid PMMA membranes, which is attributed to the crystalline moieties of PMMA. The analysis also confirmed the thermal stability of the structures up to 230 °C.

Nitrogen adsorption experiments were performed to both MIP and NIP and the physical characteristics concerning surface area, pore volume and pore diameter were calculated and presented in Table 1. The introduction of the template molecule in the imprinting process somehow influences the nucleation process during polymerization with MIP presenting lower surface area than NIP and higher average pore diameter. This is in accordance with other imprinting polymerizations reported in the literature using methacrylic acid as functional monomer and ethylene glycol dimethacrylate as cross-linker (Shi et al., 2007).

Table 2 shows the contact angles measured for each membrane. Contact angle measurements are dependent on both the hydrophilicity of the surface as well as the roughness and porosity. Hybrid membranes are shown to have higher contact angles, which is probably related with an increase in the roughness of the surfaces due to the incorporation of the highly cross-linked polymeric particles in the matrices.

The pure water flux, which is defined as the ratio between the volumetric flow rate and the membrane area and the pressure difference, is a crucial parameter in processes involving membranes. In this work we have studied the water flux through the produced membranes by ranging the hydrostatic pressure from 0 to 0.5 MPa. At these conditions the pure PMMA membrane was not permeable, even when the maximum pressure was applied. There are several parameters, which can influence the permeability of the membranes, such as hydrophilicity, porosity, pore size and interconnectivity of the pores. As it is shown in Table 2, the addition of the synthesized polymers in the casting solution for membrane preparation significantly increases the permeability of the structures. Some years ago, Merkel et al. (2002) discovered that the introduction of nonporous, fumed silica particles to high-free-volume glassy polymers significantly influenced the rearrangement of the polymer chains and could favorably increase the membrane flux. Likewise, our results show that the incorporation of imprinted polymers in the membrane scaffold can lead to increased top surface porosity and therefore reduce or eliminate the diffusional resistance.

Processes engaging membranes often require controlled mechanical loadings. In this work, DMA was used to study the viscoelastic features of PMMA and hybrid PMMA membranes. Membranes exhibited low stress break (3–4 MPa) and elongation (± 7.5% strain) in agreement with the low ductility of PMMA (Lin et al., 2006). By blending 30 wt% of NIP and MIP particles with PMMA, a slight decrease in the stress break was observed. In literature we could found some evidences that the stress break of silica composite membranes is dependent of the silica content and that for high percentages of silica, the stress break decreases, due to the agglomeration of the particles (Zou et al., 2008). Young's modulus is given by the slope of stress–strain curves and translates the stiffness of the membrane. Table 2 shows Young's modulus measured for the membranes prepared in this work. Both PMMA and hybrid PMMA membranes present an elastic behavior. The incorporation of the highly cross-linked copolymers NIP and MIP into the hybrid membranes, led to a slight decrease in Young's modulus of the structures that can be related with small differences in the porosity and pore morphology of the membranes (Barroso et al., 2009).

3.2. Template binding affinity characterization

Imprinted polymers and membranes were evaluated with respect to their ability to rebind the template molecule in aqueous solutions in static and dynamic conditions.

Batch binding experiments were performed to assess qualitatively and quantitatively the template binding affinity of the materials developed. Fig. 3 shows the experimental adsorption isotherms of template bound on both imprinted and non-imprinted materials as a function of the initial concentration of BPA. Higher adsorption of BPA was achieved by the imprinted

Table 1
Physical characteristics of NIP and MIP polymers obtained by multipoint BET method (type II).

Polymer	BET surface area (m^2 g^{-1})	Pore volume (cm^3 g^{-1})	Average pore diameter (nm)
NIP	49.8	0.072	5.8
MIP	39.8	0.070	7.0

Table 2
Physical and mechanical properties of PMMA and hybrid PMMA membranes, obtained with a thickness of 1 mm.

Membrane	Permeability (L m^{-2} h^{-1} MPa^{-1})	Contact angle (deg.)	Young's modulus (MPa)
PMMA	0[a]	46	0.539
PMMA NIP	465	91	0.419
PMMA MIP	143	94	0.437

[a] With a maximum applied pressure of 0.5 MPa.

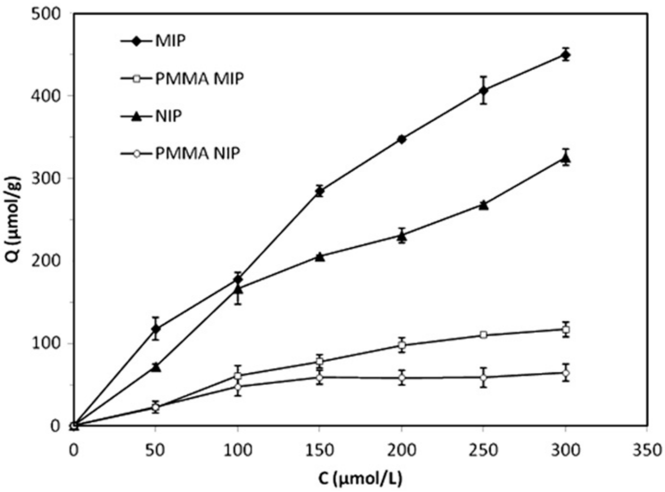

Fig. 3. Equilibrium binding curve of BPA to the synthesized polymers and membranes.

polymer reflecting an increased binding affinity to the template molecule. Polymeric powders, NIP and MIP, have higher adsorption capacity for BPA than the corresponding membranes. Adsorption of a template molecule in an imprinted membrane is dependent not only on the chemical affinity introduced by the recognition sites but also on the type of polymer, structural characteristics of the molecule, solution chemistry and membrane morphology and operating conditions. The low binding affinity of PMMA structures for BPA molecule was already reported by Ye et al. (2003). Nevertheless, the introduction of imprinted particles in the porous structure clearly increases the affinity of the membranes towards the corresponding non-imprinted hybrid membrane, as PMMA MIP is able to adsorb more BPA from the aqueous solutions than PMMA NIP.

The adsorption equilibrium data of BPA on MIP and PMMA MIP were fitted using a linearized form of the Langmuir equation, as described in the following equation:

$$\frac{1}{Q_{eq}} = \frac{1}{Q_{max}} + \frac{1}{bQ_{max}C_{eq}} \tag{4}$$

where Q_{eq} (μmol g^{-1}) is the equilibrium adsorbed amount of BPA, Q_{max} (μmol g^{-1}) is the maximum apparent binding capacity, C_{eq} (μM) is the equilibrium concentration and b (M^{-1}) is the adsorption equilibrium constant. The high correlation coefficient (0.997) obtained when fitting the MIP adsorption data with this model, suggests that adsorption takes place at specific homogeneous sites within the MIP surface. When blending the imprinted copolymer with PMMA, heterogeneity in the structure is introduced, so the correlation coefficient is lower (0.953), nevertheless a specific trend was observed due to the incorporation of MIP. Fig. 4 shows the adsorption data of BPA by MIP and hybrid PMMA MIP membrane fitted to the linearized Langmuir equation. In agreement with higher experimental adsorbed amounts, the apparent saturation capacity, Q_{max}, of MIP is higher than the saturation capacity of PMMA MIP, 625 μmol g^{-1} and 147 μmol g^{-1}, respectively. Also the binding equilibrium constant is higher for MIP, 19,950 M^{-1} versus 9190 M^{-1}. These binding properties of the imprinted materials are consistent with their affinity to the template molecule as the imprinted membrane was prepared with only 30 wt% of imprinted polymer. By tuning the amount of imprinted polymer added to the membrane cast, it should be possible to obtain hybrid membranes with different binding affinity to the template molecule.

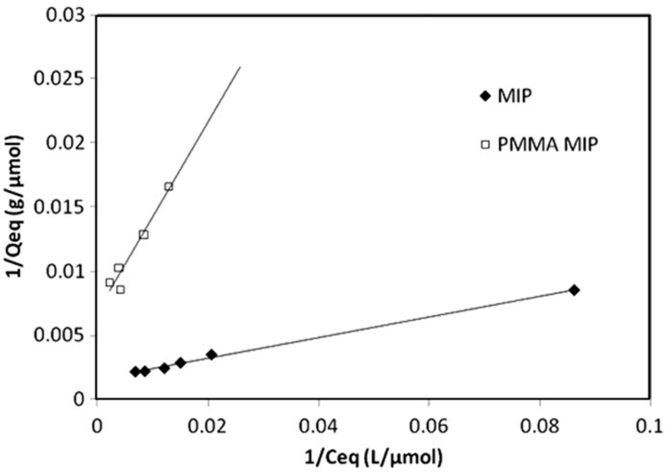

Fig. 4. Binding data for MIP and PMMA MIP fitted to a linearized Langmuir equation.

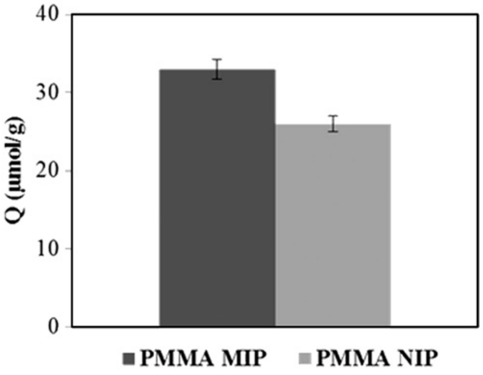

Fig. 5. BPA filtration data of hybrid membranes.

3.3. Dynamic binding of BPA

The incorporation of imprinted polymers in porous structures such as in membranes can extend the applications of these molecular recognition systems, as membranes can sense and entrap the analyte at high throughputs. The main challenge is to optimize the recognition and the membrane transport properties at the same time. Regarding dynamic binding, the amounts of BPA that hybrid membranes were able to remove from an aqueous solution with 300 μM of BPA at a flow rate of 0.33 mL min^{-1} are presented in Fig. 5. With low time of contact between membrane and template, the structures should have high recognition kinetic, so that an increased affinity adsorption could be observed. As shown, the hybrid imprinted membrane was able to adsorb a higher amount of BPA than its corresponding non-imprinted membrane. With a partial amount of imprinted particles in its structure and regarding dynamic conditions, we believe this is a promising result. Furthermore, at the end of the filtration experiments it was possible to regenerate the membrane without loss of the binding capacity.

4. Conclusions

This work demonstrates that the immobilization of imprinted polymers in a porous membrane structure, by incorporation of the functional polymers into a casting solution for membrane production is a viable method to produce affinity membranes. Moreover, the feasibility of $scCO_2$-assisted phase inversion method to prepare hybrid imprinted membranes was also attested. The main challenge when preparing imprinted membranes is to optimize both molecular recognition and membrane transport properties. Our results show these goals were achieved since the incorporation of highly cross-linked polymeric particles with molecular affinity in a porous structure considerably enhanced the affinity of imprinted membrane to the template while also increased the permeability of the PMMA membrane. This work is part of an on-going project where the materials will be tested in selectivity, in competition assays and fouling experiments. Increased efficiency is a probable outcome of future optimization work.

Based on these promising results we envisage a wide range of applications for these molecularly imprinted porous structures prepared using supercritical fluid technology, such as in bioseparations and wastewater treatment in pharmaceutical and chemical industries and sensing devices in food processing applications.

Acknowledgments

The authors would like to thank the financial support from Fundação para a Ciência e Tecnologia (FCT-Lisbon) through contracts PTDC/QUI/102460/2008, PTDC/CTM/70393/2006 and doctoral grant SFRH/BD/31085/2006 (M.S.S.), PIDDAC, FEDER, FSE and POCTI and also grant no. PEst-C/EQB/LA0006/2011.

References

Alexander, C., Davidson, L., Hayes, W., 2003. Imprinted polymers: artificial molecular recognition materials with applications in synthesis and catalysis. Tetrahedron 59, 2025–2057.

Amut, E., Fu, Q., Fang, Q., Liu, R., Xiao, A., Zeng, A., Chang, C., 2009. In situ polymerization preparation of chiral molecular imprinting polymers monolithic column for amlodipine and its recognition properties study. J. Polym. Res. 17, 401–409.

Barroso, T., Temtem, M., Casimiro, T., Aguiar-Ricardo, A., 2009. Development of pH-responsive poly(methacrylate-co-methacrylic acid) membranes using $scCO_2$ technology. Application to protein permeation. J. Supercrit. Fluids 51, 56–66.

Beltran, A., Marcé, R.M., Cormack, P.A.G., Borrull, F., 2010. Molecularly imprinted polymers: useful sorbents for selective extractions. Anal. Chim. Acta 667, 72–78.

Burridge, E., 2003. Bisphenol A: product profile. Eur. Chem. News 17, 14–20.

Casimiro, T., Banet-Osuna, A.M., Nunes da Ponte, M., Aguiar-Ricardo, A., 2005. Synthesis of highly cross-linked poly(diethylene glycol dimethacrylate) microparticles in supercritical carbon dioxide. Eur. Polym. J. 41, 1947–1953.

Cao, L., Chen, L., 2006. Influence of reaction parameters on synthesis of temperature-sensitive materials in supercritical carbon dioxide by precipitation polymerization. Polym. Bull. 57, 651–659.

Cooper, A.I., Holmes, A.B., 1999. Synthesis of molded monolithic porous polymers using supercritical carbon dioxide as the porogenic solvent. Adv. Mater. 11, 1270–1274.

de Macedo, C.V., Soares da Silva, M., Casimiro, T., Cabrita, E.J., Aguiar-Ricardo, A., 2007. Green Chem. 9, 948–953.

Dairkee, S.H., Seok, J., Champion, S., Sayeed, A., Mindrinos, M., Xiao, W., Davis, R.W., Goodson, W.H., 2008. Bisphenol A induces a profile of tumor aggressiveness in high-risk cells from breast cancer patients. Cancer Res. 68, 2076–2080.

Donato, L., Tasselli, F., Drioli, E., 2010. Molecularly imprinted membranes with affinity properties for folic acid. Sep. Sci. Technol. 45, 2273–2279.

Duarte, A.R.C., Casimiro, T., Aguiar-Ricardo, A., Simplício, A.L., Duarte, C.M.M., 2006. Supercritical fluid polymerisation and impregnation of molecularly imprinted polymers for drug delivery. J. Supercrit. Fluids 39, 102–106.

Ellwanger, A., Berggren, C., Bayoudh, S., Crecenzi, C., Karlsson, L., Owens, P.K., Ensing, K., Cormack, P., Sherrington, D., Sellergren, B., 2001. Evaluation of methods aimed at complete removal of template from molecularly imprinted polymers. Analyst 126, 784–792.

Hattori, K., Hiwatari, M., Iiyama, C., Yoshimi, Y., Kohori, F., Sakai, K., Piletsky, S.A., 2004. Gate effect of theophylline-imprinted polymers grafted to the cellulose by living radical polymerization. J. Membr. Sci. 233, 169–173.

Kho, Y.W., Kalika, D.S., Knutson, B.L., 2001. Precipitation of Nylon 6 membranes using compressed carbon dioxide. Polymer 42, 6119–6127.

Kobayashi, T., Leong, S.S., Zhang, Q.J., 2008. Using polystyrene-co-maleic acid for molecularly imprinted membranes prepared in supercritical carbon dioxide. J. Appl. Polym. Sci. 108, 757–768.

Kryscio, D.R., Peppas, N.A., 2009. Mimicking biological delivery through feedback-controlled, recognitive drug release systems based on molecular imprinting methods. AIChE J. 55, 1311–1324.

Lang, I.A., Galloway, T.S., Scarlett, A., Henley, W.E., Depledge, M., Wallace, R.B., Melzer, D., 2008. Association of urinary bisphenol A concentration with medical disorders and laboratory abnormalities in adults. J. Am. Med. Assoc. 300, 1303–1310.

Lin, D.-J., Chang, C.-L., Lee, C.-K., Cheng, L.P., 2006. Preparation and characterization of microporous PVDF/PMMA composite membranes by phase inversion in water/DMSO solutions. Eur. Polym. J. 42, 2407–2418.

Matsuyama, H., Yano, H., Maki, T., Teramoto, M., Mishima, K., Matsuyama, K., 2001. Formation of porous flat membrane by phase separation with supercritical CO_2. J. Membr. Sci. 194, 157–163.

Merkel, T.C., Freeman, B.D., Spontak, R.J., He, Z., Pinnau, I., Meakin, P., Hill, A.J., 2002. Ultrapermeable, reverse-selective nanocomposite membranes. Science 296, 519–522.

Moreira, F.T.C., Kamel, A.H., Guerreiro, J.R.L., Sales, M.G.F., 2010. Man-tailored biomimetic sensor of molecularly imprinted materials for the potentiometric measurement of oxytetracycline. Bios. Bioelectron. 26, 566–574.

Qiao, F., Sun, H., Yan, H., Row, K.H., 2006. Molecularly imprinted polymers for solid phase extraction. Chromatographia 64, 625–634.

Reverchon, E., Cardea, S., 2004. Formation of cellulose acetate membranes using a supercritical fluid assisted process. J. Membr. Sci. 240, 187–195.

Reverchon, E., Cardea, S., Rappo, E.S., 2006. Production of loaded PMMA structures using the supercritical CO_2 phase inversion process. J. Membr. Sci. 273, 97–105.

Reverchon, E., Cardea, S., 2006. PVDF-HFP membrane formation by supercritical CO_2 processing: elucidation of formation mechanisms. Ind. Eng. Chem. Res., 8939–8945.

Sergeyeva, T.A., Piletsky, S.A., Piletska, E., Brovko, O.O., Karabanova, L.V., Sergeeva, L.M., El'skaya, A.V., Turner, A.P.F., 2003. In situ formation of porous molecularly imprinted polymer membranes. Macromolecules 36, 7352–7357.

Shi, X., Wu, A., Qu, G., Li, R., Zhang, D., 2007. Development and characterisation of molecularly imprinted polymers based on methacrylic acid for selective recognition of drugs. Biomaterials 28, 3741–3749.

Soares da Silva, M., Viveiros, R., Morgado, P.I., Aguiar-Ricardo, Correia, I.J., Casimiro, T., 2011. Development of 2-(dimethylamino)ethyl methacrylate-based molecular recognition devices for controlled drug delivery using supercritical fluid technology. Int. J. Pharm. 416, 61–68.

Soares da Silva, M., Vão, E.R., Temtem, M., Mafra, L., Caldeira, J., Aguiar-Ricardo, A., Casimiro, T., 2010. Clean synthesis of molecular recognition polymeric materials with chiral sensing capability using supercritical fluid technology. Application as HPLC stationary phases. Bios. Bioelectron. 25, 1742–1747.

Takeda, K., Abe, M., Kobayashi, T., 2005. Molecular-imprinted nylon membranes for the permselective binding of phenylalanine as optical-resolution membrane adsorbents. J. Appl. Polym. Sci. 97, 620–626.

Temtem, M., Casimiro, T., Aguiar-Ricardo, A., 2006. Solvent power and depressurization rate effects in the formation of polysulfone membranes with CO_2-assisted phase inversion method. J. Membr. Sci. 283, 244–252.

Temtem, M., Casimiro, T., Mano, J.F., Aguiar-Ricardo, A., 2008. Preparation of membranes with polysulfone/polycaprolactone blends using a high pressure cell specially designed for a CO_2-assisted phase inversion. J. Supercritical Fluids 43, 542–548.

Temtem, M., Pompeu, D., Barroso, T., Fernandes, J., Simões, P.C., Casimiro, T., Rego, A.M.B., Aguiar-Ricardo, A., 2009. Development and characterization of a thermoresponsive polysulfone membrane using an environmental friendly technology. Green Chem. 11, 638–645.

Ulbricht, M., 2004. Membrane separations using molecularly imprinted polymers. J. Chromatogr. B 804, 113–125.

Van der Mare, P., Zwijnenburg, A., Kemperman, A., Wessling, M., Temmink, H., Van der Meer, W., 2010. Influence of membrane properties on fouling in submerged membrane bioreactors. J. Membr. Sci. 348, 66–74.

Wang, X., Ding, B., Sun, M., Yu, J., Sun, G., 2010. Nanofibrous polyethyleneimine membranes as sensitive coatings for quartz crystal microbalance-based formaldehyde sensors. Sensor Actuat. B-Chem. 144, 11–17.

Wei, S., Mizaikoff, B., 2007. Recent advances on noncovalent molecular imprints for affinity separations. J. Sep. Sci. 30, 1794–1805.

Ye, S., Morita, S., Li, G., Noda, H., Tanaka, M., Uosaki, K., Osawa, M., 2003. Structural changes in poly(2-methoxyethyl acrylate) thin films induced by absorption of bisphenol A. An infrared and sum frequency generation (SFG) Study. Macromolecules 36, 5694–5703.

Zou, H., Wu, S., Shen, J., 2008. Polymer/silica nanocomposites: preparation, characterization, properties and applications. Chem. Rev. 108, 3893–3957.